



Microscopic mechanism of membrane fouling in micro-filtration

Zhanping Cao^{a,*}, Jingli Zhang^b, Ligang Lin^a, Liping Xie^a

^aKey Laboratory of hollow Fiber Membrane Material and Membrane Process of Ministry of Education, Tianjin Polytechnic University, Tianjin 300387, China, Tel. +86 22 83955458; email: caozhanping2012@126.com (Z. Cao), Tel. +86 22 38955458; emails: phdlinligang@163.com (L. Lin), stpt1234@126.com (L. Xie)

^bSchool of Environmental and Municipal Engineering, Tianjin Chenjian University, Tianjin 300384, China, Tel. +86 22 23085117; email: jinglizhangczp@126.com

Received 11 November 2014; Accepted 22 January 2015

ABSTRACT

The microscopic mechanism of the membrane fouling was studied using Poiseuille equation, Langmuir adsorption model and Darcy's law. The experimental result showed that the change in membrane filtration resistance could be divided into three stages in a membrane bioreactor. The first stage was the adsorption and blocking of the membrane pore, and it is completed in a short time ($t \leq 1$ min), so it was suitable to combine its resistance with the intrinsic membrane resistance. The second stage was the change in the concentration polarization during which the resistance increased rapidly. The resistance of the concentration polarization and the resistance of the gel layer were of same character and could be united by the Langmuir relationship. The third stage had stable filtration resistance when the deposition and proliferation of the pollutants on the membrane surface achieved a dynamical equilibrium. A unified model of membrane filtration was proposed for the three stages. The experimental data of the emulsified oil wastewater filtrated by micro-membrane fitted the unified model well.

Keywords: Membrane fouling; Unified filtration model; Membrane bioreactor; Membrane pore blocking; Gel layer formation; Experimental validation

1. Introduction

In the membrane filtration process, small suspended matters in the mixed liquor can be adsorbed on the membrane surface or it can enter the membrane pore, and can cause membrane fouling and membrane flux reduction. Membrane fouling is a major obstacle in the widespread application of the membrane bioreactor (MBR). It is greatly significant to understand the process of membrane fouling for controlling it in membrane micro-filtration [1,2]. For the

stable long-term operation, the problem of membrane fouling must be fully studied, and the mathematical model of membrane fouling can provide the effective method to predict the membrane fouling. The vast literature on the hydrodynamic models of the integrated MBR are reported, and these models used at different scales mainly focus on membrane fouling [3,4]. Researchers [5–8] derived the corresponding mathematical models according to their investigation results and also used the filtration model to study the fouling characteristics [9]. But most of these models are limited to simple hydraulic factors which influences on membrane fouling [10], and few studies examined the

*Corresponding author.

membrane fouling mechanism from the entire pollution process [11]. Previous researches on membrane fouling control mainly focused on the macro-operation parameters of the reactor [12], and the micro-mechanism of membrane pollution should be studied carefully and thoroughly.

The research based on the Poiseuille equation, Langmuir adsorption theory and Darcy's law studied the micro-filtration in a submerged MBR treating municipal sewage from the micro-perspective and proposed a unified model. The experimental data of micro-membrane filtering the emulsified oil wastewater were used to validate the proposed unified model.

2. Material

2.1. Apparatus

The experimental reactor was an integrated MBR with the effective volume of 1 m³. The hollow fibre membrane module made of modified PVDF was provided by Tianjin Polytechnic University (Tianjin, China) and had total membrane area of 15 m², fibre diameter of 1.0 mm, inner diameter of 0.65 mm and membrane pore size of 0.22 μm. The air was continuously given by an air pump through perforation pipe below the membrane module. The system was schematically shown in Fig. 1.

2.2. Wastewater quality and MBR operation

Experimental influent was taken from primary sedimentation tank effluent in a sewage treatment plant (Tianjin, China). Water quality was as follows: COD 547.5 ± 38.5 mg/L; BOD₅ (384.5 ± 38.2) mg/L m; NH₄⁺-N 29.1 ± 5.4 mg/L and pH 7.3 ± 0.5. The seeding activated

sludge was taken from thickened sludge of a sludge concentration tank in a sewage treatment plant (Tianjin, China), and MLSS was approximately 5,000 mg/L. BOD sludge loading was approximately 0.24 kgBOD₅/(kgMLSS d), hydraulic retention time 5.2 h, sludge retention time 35 ± 5d; the reactor had been operated for a year. Activated sludge appeared greyish-yellow, slightly fishy and showed a good activity with the large number of Vorticella, rotifers and cilia of protozoa by microscopic examination.

3. Results and discussion

3.1. Changes of permeation flux and total resistance

The total membrane resistance is mainly comprised of membrane pore blocking resistance, membrane pore adsorption resistance, intrinsic membrane resistance, polarization resistance and gel layer resistance [13,14]. The relationship between membrane flux and the membrane filtration resistance can be expressed by Darcy's law as seen in Eq. (1).

$$J_V = \frac{\Delta P}{\mu R} = \frac{\Delta P}{\mu(R_m + R_c + R_b + R_g)} \quad (1)$$

where J_V (L/(m² h)) is the permeation flux, ΔP (Pa) is the transmembrane pressure (TMP), R (m⁻¹) is the total membrane resistance, R_m (m⁻¹) is the intrinsic membrane resistance (or clean membrane resistance), R_c (m⁻¹) is the resistance of membrane pore adsorption and blocking, R_b (m⁻¹) is the resistance which results from concentration polarization, R_g (m⁻¹) is the resistance due to gel layer formation and μ (Pa s) is the dynamic viscosity of filtered liquid.

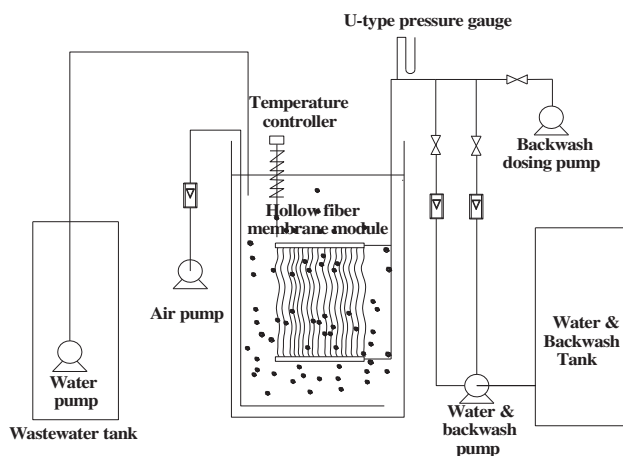


Fig. 1. The schematic diagram of MBR.

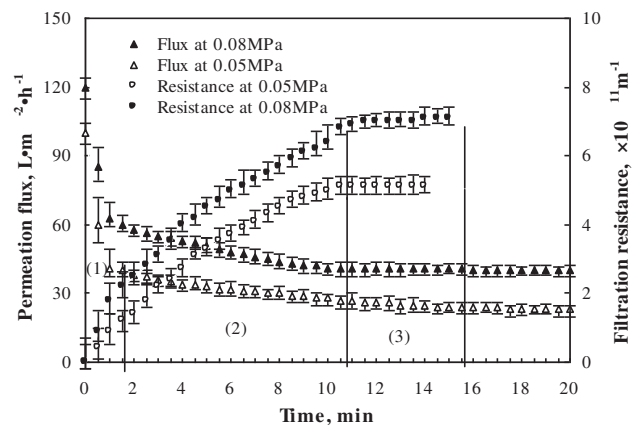


Fig. 2. Changes of permeation flux and filtration resistance with time at various transmembrane pressures.

The changes of permeation flux and total resistance were measured under constant TMP of 0.05 and 0.08 MPa (Fig. 2). According to the change of the filtration resistance, the filtering process could be divided into three stages, namely the first stage of linear rapid growth resistance, the second stage of slowdown growth resistance and the third stage of stable resistance. Corresponding to the total resistance change, the permeation flux decreased rapidly at first, then tended to be a stable value after 1 min and at last declined slightly with the extension of filtration time. The micro-mechanism of membrane fouling was discussed below.

3.2. Mechanism for linear growth of membrane pore blocking resistance at the first stage

The mixed liquor in the MBR is a non-Newtonian fluid [15], and suspended solids in the mixed liquor contain various particles in size, therefore the adsorption and jam of membrane pore and the formation of gel layer are inevitable in the membrane filtration. The standard blocking filtration model and the standard gel filtration model of non-Newtonian fluid could be used to describe this process and the former is given as

$$J_v = J_0 \exp(-K_P t) \quad (2)$$

J_0 (L/(m² h)) is the initial permeation flux, t (min) filtration time and K_P is a constant relating to membrane pore adsorption and blocking.

When $R_b=0$ and $R_g=0$, Eq. (3) is deduced from Eqs. (1) and (2),

$$\ln(R_c + R_m) = \ln R_m + K_P t \quad (3)$$

At the first stage the membrane flux declined sharply and the resistance linearly increased within 1 min. Eq. (3) was used to fit to the test data (seen as Fig. 3).

Fig. 3 shows that the test result was in good agreement with the membrane pore blocking model, and the membrane pollution was mainly caused by the membrane pore adsorption and blocking of the large molecules and particles. For the same mixed liquid, the TMP had a little effect on the membrane pore adsorption and blocking resistance, which showed that the membrane pore adsorption and blocking resistance were not dependent on transmembrane pressure. So the first stage could be called as the stage of adsorption and blocking resistance of membrane pore.

The resistance of membrane pore adsorption and blocking reached a stable value in a relatively short

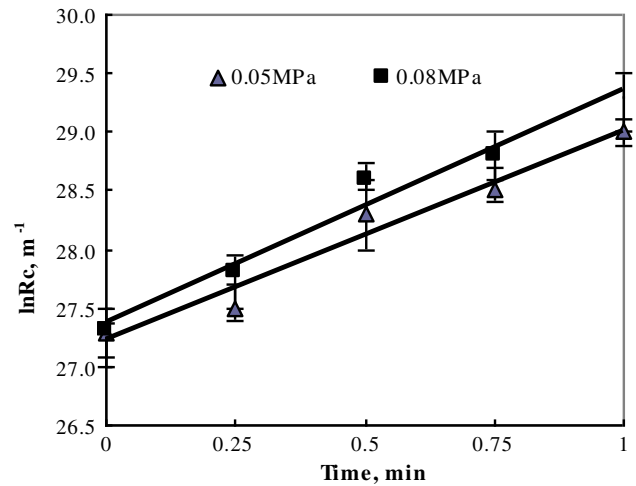


Fig. 3. Changes of membrane adsorption and blocking resistance with time.

time ($t \leq 1$ min), and it could be regarded as a constant. Due to the boundary layer of membrane surface, the water flow in the membrane pore could be Laminar flow. Membrane pore could be expressed as a cylinder vertical to membrane surface with the effect of curvature factor to be considered. The intrinsic membrane resistance can be given by the Poiseuille equation [16] as

$$J_v = \frac{\Delta P}{R_m} = \frac{\varepsilon_1 r^2 \Delta P \rho}{8 \phi^2 \mu \delta_m} \quad (4)$$

where ε_1 (%) is the membrane porosity, δ_m (m) is the membrane thickness, ϕ (%) is the curvature factor, ρ (kg/m³) is fluid density and r (m) is the membrane pore radius.

At the initial stage of filtration, particles smaller than the membrane pore in size might flow through the membrane in theory when they enter into the pore, but because of the membrane pore tortuosity and the inertial force part of could be divorced from the streamline and contacted with the pore wall, and attached to the pore wall under Van der Waals' force and electrostatic interaction. Meanwhile, the attached particles underwent a shear force, which caused them to shed. K_P must be a function of the curvature factor and the pore size. The experiment data showed that the adsorption speed and the shedding speed reached the equilibrium in 1 min (Fig. 1), and the adsorption and blocking resistance of membrane pore reached a steady state and increased a little with the extension of filtration time. Membrane blocking is completed in a relatively short time; therefore, it was suitable to

combine the resistance of membrane pore adsorption and blocking with the intrinsic membrane resistance as the modified intrinsic membrane resistance R'_m . R'_m is expressed as:

$$R'_m = R_m \exp(K_P t) \quad t \leq 1 \text{ min} \quad (5)$$

And then Eq. (1) is also described as

$$J_V = \frac{\Delta P}{\mu(R'_m + R_b + R_g)} \quad (6)$$

3.3. Resistance characteristics of polarization and gel layer at the second and third stage

In the MBR aerated below the membrane module, when the membrane surface is not completely covered by small particles, the second layer fine particles in the boundary layer could move to a monolayer distribution because of the shear force caused by aeration. So, the gel layer formation accords with the Langmuir adsorption theory.

Coverage (θ) is defined as the percentage of the area of fine particles on membrane surface and that of the membrane surface. The fraction $(1-\theta)$ of the membrane surface is not covered by fine particles. The radial migration rate of fine particles to the membrane surface is in direct proportion to the TMP ΔP , so radial migration rate $= k_1 \Delta P$, where k_1 is a proportional factor.

The diffusion rate of fine particles is directly proportional to the coverage (θ) of particle on the membrane surface, and Brown diffusion coefficient (k_2) is given by the Stokes-Einstein equation, so the diffusion rate $= k_2 \theta$.

When the two rates reaches to a dynamic balance they are equal, $k_1 \Delta P = k_2 \theta$. Let

$$\frac{k_1}{k_2} = \Phi, \text{ it is gotten as } \theta = \Phi \Delta P \quad (7)$$

where Φ is called the sedimentation equilibrium constant and is relative with the particle size, the suspended solid concentration, the temperature and the viscosity of mixed liquor.

With the increase in transmembrane pressure, θ rose as seen from Eq. (7), i.e. the membrane surface covered with particles increases. With the aggravation of concentration polarization, the filtration resistance increases. When θ reaches to 1 the gel layer is formed, the concentration polarization resistance R_b is converted into the gel layer resistance R_g and the limit of

the polarization resistance is the gel layer resistance. Before θ reaches to 1 the relationship between the concentration polarization resistance and the gel layer resistance can be described as $R_b = \theta R_g$, which indicated that the filtration resistance is the value of the concentration polarization resistance, and the concentration polarization resistance and the gel layer resistance are of the same nature. After θ is equal to 1 the fine particles deposited on the surface of the first gel layer continually, and the gel layer thickness increases.

During the course from concentration polarization to gel layer formation (i.e. the process which θ increases to 1), the concentration polarization resistance is a function of TMP ΔP and can be expressed as

$$R_b = R_g \Phi \Delta P \quad (8)$$

Based on the polarization–gel layer model of Langmuir adsorption theory, Darcy's law can be further written as

$$J_V = \frac{\Delta P}{\mu(R'_m + \theta R_g)} \quad (9)$$

The viscosity of mixed liquor is considered to distribute the resistance term, so $\mu R'_m$ can be denoted as R''_m and $\mu \Phi R_g$ as $\Phi R'_g$. Therefore, before the gel layer formation Eq. (9) can be rewritten as

$$J_V = \frac{\Delta P}{R''_m + \Phi R'_g \Delta P} \quad (10)$$

When the TMP ΔP increases to a certain extent and $\Phi R'_g \Delta P$ is far larger than the modified intrinsic membrane resistance R''_m , the membrane flux is not dependent on the pressure, the gel layer is formed ($\theta=1$) and the permeation flux reaches to the limit. $J_{V\text{Lim}}$ can be calculated by

$$J_{V\text{lim}} = \frac{1}{\Phi R'_g} \quad (11)$$

And Eq. (10) is expressed as

$$J_V = \frac{\Delta P}{R_m + \frac{1}{J_{V\text{lim}}} \Delta P} \quad (12)$$

The limit flux is related to contaminant concentration, particle size, liquid viscosity and temperature, namely the characteristics of the filtering liquid, and not to

the transmembrane pressure. And Agashichev [17] also thought that gel properties are independent of applied pressure. This model is consistent with the experimental data.

4. Validation of the unified model

4.1. Experiment

In order to validate the above unified model, the filtration treatment for emulsified oil wastewater was studied in a submerged membrane device the same as Fig. 1. The three different concentrations of lubricating oil and water (m/m), 0.1%, 1% and 5%, were prepared as follows: added common machine lubricating oil (JUSTAR 700U, China Sinopec Lubricating Oil Co., Ltd.) and a small amount of emulsifier with hydrophile-lipophile balance value between 12 and 14 (polyoxyethylene nonylphenol ether, OP-10) into distilled water, stirred at low-speed of 200 rpm for 10 min and then high-speed of 3,000 rpm for 30 min by electric mixer. The lubricating oil and water formed a stable emulsion, and the size of most oil drops were at the range of 0.1 to 4 μm .

4.2. Experimental data and analysis

The changes of membrane flux are shown in Fig. 4 under the various TMP for the three content of emulsified oil wastewater.

At the emulsified oil content of 0.1%, the membrane flux could not reach to the maximum under the experimental transmembrane pressure, that is to say, the limit flux was very large. Therefore, $\frac{1}{R'_m} \Delta P \approx 0$ and Eq. (12) was expressed as $J_V = \frac{\Delta P}{R'_m} J_V$ was

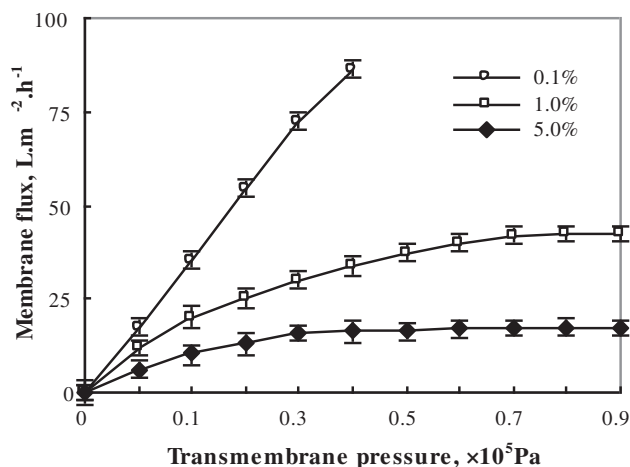


Fig. 4. Membrane flux with TMP for three different content of emulsified oil wastewater.

proportional to ΔP and the experimental data were in agreement with the model.

At the emulsified oil content of 1% and 5% with the increase of the TMP the membrane flux rose linearly and rapidly at first, and then the membrane flux grew slowly. Finally, the membrane flux reached to a stable value. It is also seen from Fig. 4 that the limit flux was 42.1 $\text{L}/\text{m}^2 \text{ h}$ at emulsified oil content of 1%, and the limit flux was 18.2 $\text{L}/\text{m}^2 \text{ h}$ at the emulsified oil content of 5%. When the content of emulsified oil was higher, the limit membrane flux and the TMP that reached to the limit flux were smaller and θ reached to 1 more quickly. It was concluded from Eq. (7) that Φ rose rapidly with the increase of emulsified oil content. The limit flux is determined by Φ and has nothing to do with the transmembrane pressure. The liquid characteristics are decisive factors that affect the membrane flux.

4.3. Determination of J_V and R'_m in the unified model

Eq. (13) can be obtained from Eq. (12) after the gel layer is formed.

$$\frac{1}{J_V} = R'_m \frac{1}{\Delta P} + \Phi R'_g \quad (13)$$

A linear regression was performed between the two variables, $\frac{1}{J_V}$ and $\frac{1}{\Delta P}$, for the various concentration of emulsified oil wastewater. The linear correlation coefficients R^2 were larger than 0.98 and the significance level α were smaller than 0.01, which implies that there is statistically significant correlation between the two variables (as seen in Fig. 5). The regression equation was used to calculate straight slope (R''_m) and intercept ($\Phi R'_g$). And then $J_{V\text{lim}}$ was obtained by Eq. (11). $J_{V\text{lim}}$ and R''_m were more than 1,000 $\text{L}/(\text{m}^2 \text{ h})$ and $2.7 \times 10^2 \text{ h Pa m}^2/\text{L}$, 42.1 $\text{L}/(\text{m}^2 \text{ h})$ and $3.2 \times 10^2 \text{ h Pa m}^2/\text{L}$ and 18.5 $\text{L}/(\text{m}^2 \text{ h})$ and $4.1 \times 10^2 \text{ h Pa m}^2/\text{L}$ at the emulsified oil concentration of 0.1%, 1% and 5%, respectively.

The membrane flux equation is obtained as Eq. (14) at the emulsified oil content of 1%.

$$J_V = \frac{\Delta P}{3.2 \times 10^2 + \frac{1}{42.1} \Delta P} \quad (14)$$

when $\frac{\Delta P}{42.1}$ is 10 times or more of the corresponding R'_m , J_V is not dependent on the TMP ΔP , and the gel layer has formed. The increase in TMP reflected the gel layer thickening and the pressure increased was offset by a gel layer resistance R_g , so the limit flux remains constant.

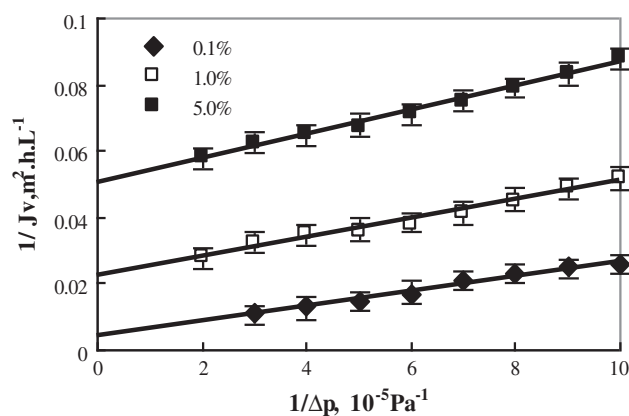


Fig. 5. Relations between $\frac{1}{J_v}$ and $\frac{1}{\Delta p}$.

It is found that the experimental data are consistent with Eq. (12) when the resistance of membrane pore adsorption and blocking is combined with the intrinsic membrane resistance and the viscosity of mixed liquor is also considered.

5. Conclusions

- (1) The intrinsic membrane resistance could be combined to the membrane pore blocking resistance, and the modified pore filtration resistance could be expressed as $R'_m = R_m \exp(K_p t)$ ($t \leq 1 \text{ min}$).
- (2) The mathematical model of membrane filtration resistance could be unified as $J_v = \frac{\Delta p}{R^v + \Phi R'_g \Delta p}$ and $J_{v \text{ lim}} = \frac{1}{\Phi R'_g}$ by using Poiseuille equation, Langmuir adsorption model and Darcy's law in the MBR.
- (3) The limit flux was not dependent on trans-membrane pressure, but on the characteristics of the filtered liquid.
- (4) The experimental data of the emulsified oil wastewater filtrated by micro membrane fitted the unified model well.

Acknowledgments

This work was supported by the National Natural Science Foundation of China (No. 51078265) and Ministry of Housing and Urban-Rural Development of China (No. 2014-K7-004).

References

- [1] I.M. Griffiths, A. Kumar, P.S. Stewart, A combined network model for membrane fouling, *J. Colloid Interface Sci.* 432 (2014) 10–18.
- [2] Q. Yang, X. Huang, H.T. Shang, X.H. Wen, Y. Qian, Resistance analysis for recirculated membrane bioreactor, *Environ. Sci.* 27 (2006) 2344–2349 (in Chinese).
- [3] W. Naessens, T. Maere, I. Nopens, Critical review of membrane bioreactor models—Part 1: Biokinetic and filtration models, *Bioresour. Technol.* 122 (2012) 95–106.
- [4] W. Naessens, T. Maere, N. Ratkovich, S. Vedantam, I. Nopens, Critical review of membrane bioreactor models—Part 2: Hydrodynamic and integrated models, *Bioresour. Technol.* 122 (2012) 107–118.
- [5] R. Liu, X. Huang, Y.F. Sun, Y. Qian, Hydrodynamic effect on sludge accumulation over membrane bioreactor, *Process Biochem.* 39 (2003) 157–163.
- [6] Y. Shimizu, Y.I. Okuno, K. Uryu, S. Ohtsubo, A. Watanabe, Filtration characteristics of hollow fiber microfiltration membranes used in membrane bioreactor for domestic wastewater treatment, *Water Res.* 30 (1996) 2385–2392.
- [7] R. Bai, H.F. Leow, Microfiltration of activated sludge wastewater—the effect of system operation parameters, *Sep. Purif. Technol.* 29 (2002) 189–198.
- [8] M.F.R. Zuthi, H.H. Ngo, W.S. Guo, Modelling bioprocesses and membrane fouling in membrane bioreactor (MBR): A review towards finding an integrated model framework, *Bioresour. Technol.* 122 (2012) 119–129.
- [9] S.J. Lee, M. Dilaver, P.K. Park, J.H. Kim, Comparative analysis of fouling characteristics of ceramic and polymeric microfiltration membranes using filtration models, *J. Membr. Sci.* 432 (2013) 97–105.
- [10] A. Boyle-Gotla, P.D. Jensen, S.D. Yap, M. Pidou, Y. Wang, D.J. Batstone, Dynamic multidimensional modelling of submerged membrane bioreactor fouling, *J. Membr. Sci.* 467 (2014) 153–161.
- [11] A. Abdelrasoul, H. Doan, A. Lohi, A mechanistic model for ultrafiltration membrane fouling by latex, *J. Membr. Sci.* 433 (2013) 88–99.
- [12] M.J. Kim, B. Sankararao, C.K. Yoo, Determination of MBR fouling and chemical cleaning interval using statistical methods applied on dynamic index data, *J. Membr. Sci.* 375 (2011) 345–353.
- [13] T.W. Cheng, H.W. Yeh, C.T. Cau, Resistance analyses for ultrafiltration in tubular membrane module, *Sep. Purif. Technol.* 32 (1997) 2623–2640.
- [14] A.K. Pabby, Handbook of Membrane Separations: Chemical, Pharmaceutical and Biotechnological Applications, CRC Press, New York, NY, 2008.
- [15] S. Rosenberger, K. Kubin, M. Kraume, Rheology of activated sludge in membrane bioreactors, *Eng. Life Sci.* 2 (2002) 269–275.
- [16] J.M. Michael, C. Orr, Filtration: Principles and Practices, Marcel Dekker, INC, New York, NY, 1987.
- [17] S. Agashichev, Modelling non-Newtonian behaviour of gel layers at membrane surfaces in membrane filtration, *Desalination* 113 (1997) 235–246.